Available online at www.sciencedirect.com
SCIENCE DIRECT®
Physica A 329 (2003) 451–458
PHYSICA A
www.elsevier.com/locate/physa

Improving the realism of the cellular Potts model in simulations of biological cells

Noriyuki Bob Ouchi[a], James A. Glazier[b], Jean-Paul Rieu[c,*], Arpita Upadhyaya[d], Yasuji Sawada[e]

[a] *Radiation Risk Analysis Laboratory, Department of Health Physics, JAERI, Tokai, Ibaraki 319-1195, Japan*
[b] *Biocomplexity Institute, Department of Physics, Swain Hall West 159, 727 East Third Street, Bloomington, IN 47405-7105, USA*
[c] *Laboratoire de Physique de la Matière Condensée et Nanostructures, Department de Physique des Materiaux, Universite Claude Bernard-Lyon I, 43 Boulevard du 11 Novembre 1918, Villeurbanne, Cedex 69622, France*
[d] *Department of Mechanical Engineering, Massachusetts Institute of Technology, 77 Massachusetts Avenue, Cambridge, MA 02139, USA*
[e] *Tohoku Institute of Technology, Yagiyama-kasumicho 35-1, Taihaku-ku, Sendai 982-8577, Japan*

Received 17 December 2002

Abstract

Because the extended or cellular large-Q Potts model (CPM) captures effectively the global features of tissue rearrangement experiments, including cell sorting and tissue engulfment, it has become a common technique for cell level simulation of tissues. However, it omits three key elements of real cells, their fixed membrane area, their attractive binding and the dissipation of making and breaking membrane contacts. In this paper, we modify the Hamiltonian to use negative surface energies, constrained surface area and a spin flip energy threshold to improve the correspondence to reality. We find that the new model correctly predicts several dynamical behaviors of cells which the original CPM does not, including the hierarchy of diffusion constants.

PACS: 87.18.Ed; 87.17.Jj; 87.15.Vv; 05.90.+m

Keywords: Potts model; Diffusion; Cell motion

* Corresponding author. Tel.: +33-4-72-44-82-28; fax: +33-4-72-43-29-25.
E-mail addresses: glazier@indiana.edu (J.A. Glazier), rieu@lpmcn.univ-lyon1.fr (J.P. Rieu).

0378-4371/$ - see front matter © 2003 Published by Elsevier B.V.
doi:10.1016/S0378-4371(03)00574-0

1. Introduction

In 1962 Steinberg proposed that differences in cell–cell adhesion energies (differential adhesion) could explain many patterns observed *in vitro* and during development [1]. This fundamental observation has inspired a number of energy-based models of tissues including the cellular large-Q Potts model (CPM). When multiple types of cells from a primitive animal or an embryo are dissociated, randomly intermingled and then re-aggregated, they re-establish coherent homotypic domains, the less cohesive types forming layers surrounding the more cohesive types. This *cell sorting* offers insight into the mechanisms governing morphogenesis. Sorting has long been studied using organisms including *hydra* [2]. Numerical simulations of cell sorting using the CPM started almost a decade ago [3,4]. They showed that random cell fluctuations and differential adhesion between different cell types suffice to simulate various biological phenomena, including cell sorting, tissue engulfment and tissue rounding. Potts model simulations can also describe nonbiological phenomena like grain growth [5] and foam rheology [6]. The predictive power of the CPM goes remarkably far: the CPM plus reaction-diffusion equation can describe the entire life cycle of the slime mould *Dictyostelium discoideum* [7].

Because of its flexibility and simplicity of implementation, CPM methods are increasingly common in complex biological simulations [8–11]. However, the model parameters do not correspond directly to important experimental properties and the dependence of the simulation on its own parameters has not been studied systematically. While certain scalings, e.g. energy/temperature have unambiguous meanings, the parameters generally have complex nonlinear interactions which make dimensional arguments for parameter dependencies difficult or impossible. Here we investigate some of these dependencies to provide guidance for parameter tuning.

All models are compromises between simplicity and realism. The standard CPM works surprisingly well for many purposes, even though it neglects three fundamental aspects of cell behavior: that cell membrane interactions are attractive, that the total amount of cell membrane is fixed and that making and breaking membrane contacts is dissipative. In this paper we extend the CPM to include these biological effects and find that we then correctly predict the hierarchy of diffusion constants in experiment, which the standard CPM gives incorrectly.

Recently, we characterized cell motion in different types of cohesive aggregates to elucidate the role of adhesion in cell motion [12]. We used confocal microscopy to study the center of mass displacements and membrane deformations of single endodermal *hydra* cells in ectodermal and endodermal 2D aggregates. Here, the endodermal aggregates are the more cohesive [13,14]. In both types of aggregate, cells perform a persistent random walk, with the diffusion constant smaller in endodermal aggregates. The cell deformations are random, with their amplitude and direction uncorrelated with the center of mass motion. The random forces exerted by the surrounding cells predominate over the deformations of the cell itself, displacing the cell within the aggregate [12]. In this paper, we examine quantitatively the extensions of the CPM required to simulate these experimental results and show that negative values for the surface energy are essential. We also study systematically the influence of the overall parameters

on the cell motion over a wide range determined by the following two requirements: (i) cells should move diffusively (i.e., they do not trap) and (ii) they should not split. In a future paper we will explicitly constrain the velocity autocorrelation of cell motion and compare the results to experimentally observed large scale flows [15].

2. The CPM

The CPM [3], assigns a spin σ_{ij} to each lattice site, (i,j). The set of all sites with the same spin, σ, defines a cell. Each cell has an associated cell type, τ. The energy per unit surface area depends on cell type, $J_{\tau\tau'}$. We introduce three cell types, $\tau \in \{l,d,m\}$, where l denotes the less cohesive light cells which we compare to ectodermal cells in *hydra* experiments, d denotes the dark cells (i.e., endodermal cells), and m the culture medium. In 2D simulations, we introduce the cell volume and membrane area as a target area A_τ and a target perimeter l_τ. The latter modifies previous simulations [3] to model the fixed amount of membrane in each cell. It also prevents the splitting of cells into many subcells in the case of negative surface energies J. Thus, the total energy is:

$$H = \sum_{(ij)-(i'j')} J_{\tau\tau'}(1-\delta_{\sigma,\sigma'}) + \left\{ \lambda_1 \sum_{\sigma} (a(\sigma)-A_\tau)^2 + \lambda_2 \sum_{\sigma} (l(\sigma)-l_\tau)^2 \right\} (1-\delta_{\tau,m}) \,, \tag{1}$$

where $a(\sigma)$ and $l(\sigma)$ are, respectively, the area and perimeter of cell σ, and λ_1 and λ_2 are the elasticity parameters. At each step, we apply the Metropolis algorithm, choose a site at random and accept a proposed change in its spin value with a Boltzmann transition probability dependent on temperature $T > 0$:

$$P = \{\exp(-(\Delta H - H_0)/T) : \Delta H > H_0;\ 1 : \Delta H < H_0 \,, \tag{2}$$

where H_0 is a threshold for a spin flip adopted from Hogeweg et al. [10].

In the original Potts model for grain growth, the surface energies were positive because grain boundary cost energy. Choosing positive energies might seem natural in the biological case as well, because the cells try to minimize their surface area, while for negative surface energies the cells tend to fall apart to create the maximum possible surface area. Thus, for positive surface energies a cell can reduce its surface energy by creating dark–dark or light–light boundary at the expense of dark–light boundary and by making all boundaries as short as possible. However, real cells are cohesive, i.e., they *reduce* their energy by binding, while their total membrane area remains constant. Thus we should constrain the binding energy and surface area separately, rather than jointly using a single term. In the case of fluids, a negative contact energy corresponds to miscible fluids which do indeed maximize their contact area (it goes to infinity) in the absence of any surface area constraint.

We choose both positive and negative surface energies to satisfy the sorting condition that the corresponding surface tensions [4] should satisfy $\gamma_{dm} > \gamma_{dl} + \gamma_{lm}$ and the other

parameters to ensure complete sorting, to mimic the situation in most simulations. We use a square lattice of 128×128 sites. The number of the neighboring sites is 8. We examine diffusion of single cells of either type in homogeneous aggregates of either type with periodic boundary conditions (256 cells with a target size of 64 pixels). For a given aggregate, we calculate the mean-squared displacement (MSD) of one cell as a function of the time interval t:

$$\langle \rho^2(t) \rangle = \langle (x_i(t_0 + t) - x_i(t_0))^2 + (y_i(t_0 + t) - y_i(t_0))^2 \rangle \,, \tag{3}$$

where we take the average over 16 ensembles and over all possible t_0 using overlapping intervals [16]. The slope of the MSD for short times gives the diffusion constant [16]. We also compute the velocity autocorrelation function $C(t) = Z(t)/Z(0)$ with $Z(t) = \langle \vec{v}_i(t_0 + t) \cdot \vec{v}_i(t_0) \rangle$, where $\vec{v}_i$ is the velocity calculated using a time step interval $\Delta t = 1$ MCS.

3. Statistical calculations

We first use the same positive surface energies as in previous simulations ($T = 5$, $J_{ll} = 14$, $J_{dd} = 2$, $J_{dl} = 11$, $J_{dm} = J_{lm} = 16$, $A_l = A_d = 20$, $H_0 = 0$, $\lambda_1 = 1$ and $\lambda_2 = 0$). The surface tensions [4], are, respectively, $\gamma_{ld} = 3$, $\gamma_{lm} = 9$ and $\gamma_{dm} = 15$. Light aggregates have a lower surface tension with external medium than dark aggregates, corresponding to their lower cohesion. The MSDs of a dark cell in both light and dark aggregates are linear, indicating normal diffusion. Since diffusion occurs mainly by creating and destroying units of surface area rather than by replacing a unit of light surface by a unit of dark surface, we expect that the energy threshold for cell movement will be higher for larger absolute values of surface energy (with respect to zero). Thus, in the CPM, we expect more cohesive cells to diffuse faster than less cohesive cells for positive energies and slower for negative energies. The expected result for positive energies is opposite to our common sense that diffusion should be faster in less cohesive aggregates and also to our experimental results: in *hydra* aggregates, endodermal cells move faster in ectodermal aggregates than in more cohesive endodermal aggregates [12]. As expected from theoretical considerations, the diffusion constant is lower in the less cohesive light aggregate than in the more cohesive dark aggregate. In order to recover the correspondence with experimental results [12], we must use negative surface energies. The final equilibrium pattern, however, depends only on the energy differences between the various Es and not on the value of zero energy.

We therefore use the following parameters: $T = 10$, $J_{ll} = -5$, $J_{dd} = -25$, $J_{ld} = -3$, $J_{lm} = 1$, $J_{dm} = 20$, $H_0 = 0$, $\lambda_1 = 10$, $A_l = A_d = 260$, $\lambda_2 = 5.5$, $l_l = l_d = 65$. Although we use negative energies, the surface tensions are positive with a larger value for the dark/medium interface: $\gamma_{ld} = 12$, $\gamma_{lm} = 3.5$ and $\gamma_{dm} = 32.5$. We first carefully checked that the chosen surface energies ensured complete sorting, matching simulations with positive energies [4] or experiments with *hydra* aggregates [13] (data not shown). For negative energies a dark cell in a light aggregate should move more quickly than in a dark aggregate. Fig. 1 shows that the MSD of dark cells is larger in light aggregates as found in experiments [12]. Fig. 2a summarizes the influence of the surface energy $J_{\tau\tau}$

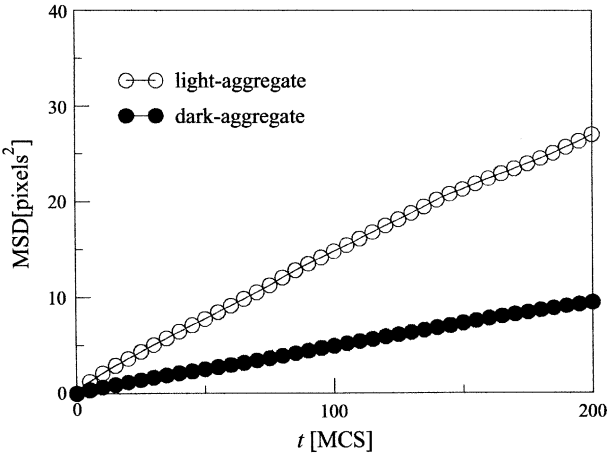

Fig. 1. Mean squared displacement (MSD) of a dark cell in a dark aggregate d (bullets) and in a light aggregate l (circles) using negative surface energies. The simulation used the following parameters: $T = 10$, $H_0 = 0$, $J_{ll} = -5$, $J_{dd} = -25$, $J_{dl} = -3$, $A_l = A_d = 64$, $l_l = l_d = 35$, $\lambda_1 = 10$ and $\lambda_2 = 5.5$. We averaged 16 cells in one simulation for this calculation.

on homogeneous aggregates: the diffusion constant D decreases as $J_{\tau\tau}$ decreases (i.e., as the cohesiveness increases). Experimentally, we always found a short persistence time for the motion of cells within aggregates [12].

In simulations, we computed the autocorrelation function of the velocity for both positive and negative surface energies. The autocorrelation function always exhibits a negative peak at short times and then reaches zero rapidly as in Fig. 3 (curve with $H_0 = 0$). At long times, velocities are uncorrelated ($C(t) = 0$), consistent with a random walk. Thus, the main difference between the simulation and experiment for *hydra* aggregates is in short time behavior. The autocorrelation is always positive experimentally and fits roughly a decaying exponential, indicating persistence in the cell motion at short times [12], while, the autocorrelation is negative at short times in simulations, indicating that when a cell moves and deforms in some direction it has a large probability to recover its initial position and shape. The cell center of mass thus oscillates.

These oscillations have a simple explanation. The Metropolis algorithm makes zero energy changes with probability one. Since spin flips are reversible, the probability for a spin to flip to a new value and then return to its old value at the next flip is very high, limited only by the probability that another spin flip at a different location will decrease the spin flip probability ($P < 0.5$). Thus, the most likely event after a zero or positive energy flip is to return to the initial condition.

The Metropolis algorithm is appropriate for a conservative system, like a magnet, but not to cells, where the formation and the destruction of bonds is highly dissipative. We can make our model more realistic by setting a threshold H_0 for a spin flip higher than zero to reflect this dissipation [10]. In Fig. 3, we plot the velocity autocorrelation as a function of the threshold. Increasing the threshold to $H_0 = 80$

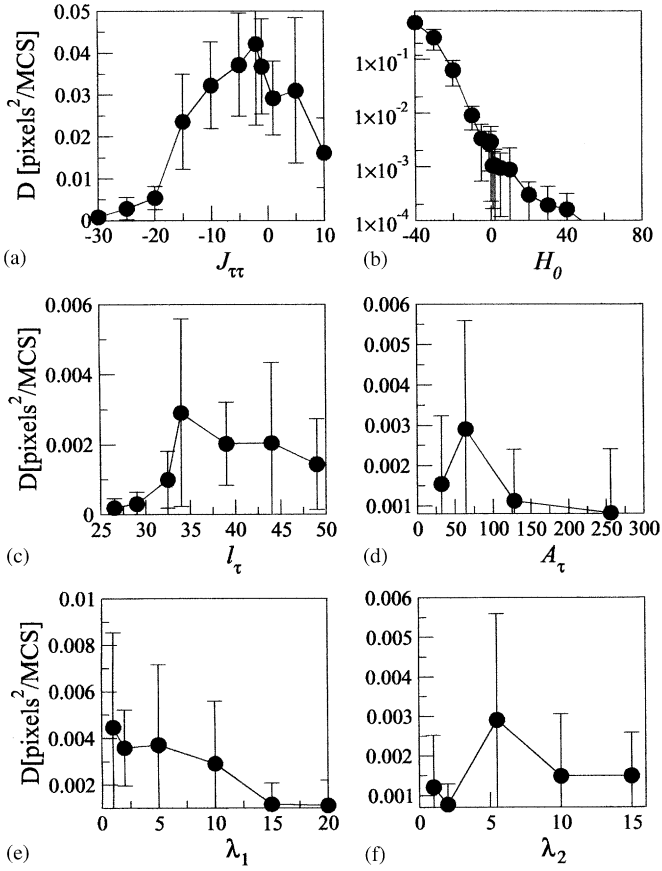

Fig. 2. Diffusion constant as a function of (a) surface energy $J_{\tau\tau}$ in homogeneous aggregates, (b) threshold for spin flip H_0, (c) target perimeter l_τ, (d) target area A_τ with $l_\tau = 2\pi\sqrt{a_\tau/\pi}$, (e) area constraint λ_1 and (f) perimeter constraint λ_2. For each curve, remaining parameters take the following default values: $T = 10$, $H_0 = 0$, $J_{\tau\tau} = -25$, $A_\tau = 64$, $l_\tau = 35$, $\lambda_1 = 10$ and $\lambda_2 = 5.5$.

eliminates the autocorrelation negative peak. Hogeweg et al. [10] introduced thresholding to suppress oscillations in the CPM, but did not study its effect systematically. Using negative energies, the oscillations vanish both at large positive and negative values of the threshold H_0 (see inset of Fig. 3), since positive H_0 suppresses energetically favorable flips and negative H_0 suppresses the return flip. Increasing H_0 decreases the diffusion constant exponentially for both positive and negative surfaces energies (Fig. 2b) because a larger H_0 exponentially suppresses positive energy and neutral energy boundary motion, and diffusion is an energetically neutral process.

The influence of the cell size and cell shape on the diffusion constant is easy to understand. When increasing the target perimeter l_τ at a given target area ($A_\tau = 64$), D first strongly increases (Fig. 2c). The first value investigated $l_\tau = 29$ corresponds

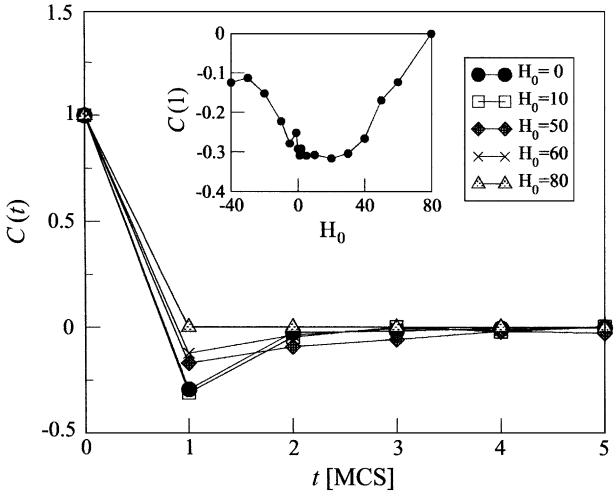

Fig. 3. Autocorrelation function of the velocity of a dark cell in a dark aggregate as a function of the non-normalized threshold value H_0 for spin flips. We calculated the velocity using negative surface energies with $\Delta t = 1$ MCS. Inset is the plot of minimum values of the autocorrelation function of the velocity, $C(1)$, as a function of H_0. The simulation used the following parameters: $T = 10$, $J_{\tau\tau} = -25$, $A_\tau = 64$, $l_\tau = 35$, $\lambda_1 = 10$ and $\lambda_2 = 5.5$.

roughly to the perimeter of a circle of area 64 pixels. The cell contour is very tight, forcing cells to be nearly circular. Smaller values of l_τ will tend to shrink the cell and increase its internal pressure, making it increasingly rigid. The value $l_\tau = 35$ at the maximum of D corresponds roughly to 20% excess perimeter with respect to a perfectly circular perimeter. For larger target perimeters, D decreases slightly, as cells become soft and start to split into small pieces. These small pieces have very large boundary curvatures and hence adding pixels to their surface has a higher energy cost in terms of the number of mismatched bonds per pixel than for larger cells. The result is that the fragment's center of mass mobility decreases (see Fig. 2d). We use 20% excess perimeter in what follows.

In particular, we evaluate the influence of the target area A_τ on D. For very small target areas, the curvature effect mentioned above decreases the mobility. For large target areas, increasing the target area reduces the diffusion constant (Fig. 2d). Each one pixel fluctuation moves the center of mass by a distance $1/A_\sigma$, while the number of surface pixels increases like $\sqrt{A_\sigma}$, so for a bigger cell, the cell center of mass movement decreases as $1/\sqrt{A_\sigma}$.

The diffusion constant strongly depends on the area constraint λ_1 (Fig. 2e). As the area constraint increases, D decreases. The effect is the same as when the target perimeter decreases; the cells become more rigid. For very small values of the perimeter constraint, λ_2, cells split, causing curvature reduction of D. Large values of λ_2 increase cell rigidity and reduce D (Fig. 2f). For values of λ_2 larger than 10, the MSDs are not linear but have a $t^{1/2}$ form, meaning that the cells often trap in particular metastable

configurations because fluctuations cost too much energy. Thus, the plots of D as a function of parameters, λ_2, l_τ, and A_τ have maxima where the trade off between fragmentation/curvature inhibition and rigidity inhibition is optimal. We predict that experimenters will find that real cells operate in this range. The results of Figs. 2d–f for negative surface energies also hold for positive energies.

4. Conclusion

Based on our recent quantitative experiments on single cell motion in aggregates [12,13] we have improved the realism of the CPM. Previous CPM simulations using positive energies [3,4] captured effectively the global features of tissue rearrangement but failed to describe their dynamics correctly. Modifying the Hamiltonian to use negative surface energies, constraining the membrane area and introducing a spin flip energy threshold improve the correspondence to experiments and preserve desirable qualitative behaviors. Optimization of the other parameters requires careful tuning due to the competition between cell splitting and cell rigidity.

Acknowledgements

We acknowledge support from Grants NSF-INT96-03035-OC, NSF-INT98-02417, NSF-IBN-0083653 and the Japanese Grant-in-Aid for Science Research Fund from the Ministry of Education, Science and Culture (No. 08409002, 40020400).

References

[1] M.S. Steinberg, Proc. Nat. Acad. Sci. USA 48 (1962) 1577;
M.S. Steinberg, Science 137 (1962) 762.
[2] P. Armstrong, Crit. Rev. Biochem. Mol. Biol. 24 (1989) 119.
[3] F. Graner, J.A. Glazier, Phys. Rev. Lett. 69 (1992) 2013.
[4] J.A. Glazier, F. Graner, Phys. Rev. E 47 (1993) 2128.
[5] J.A. Glazier, Phys. Rev. Lett. 70 (1993) 2170.
[6] F. Elias, C. Flament, J.A. Glazier, F. Graner, Y. Jiang, Philos. Mag. B 79 (1999) 729.
[7] A.F. Marée, P. Hogeweg, Proc. Nat. Acad. Sci. USA 98 (2001) 3879.
[8] H. Levine, I. Aranson, L. Tsimring, T.V. Truong, Proc. Nat. Acad. Sci. USA 93 (1996) 638.
[9] Y. Jiang, H. Levine, J.A. Glazier, Biophys. J. 75 (1998) 2615.
[10] P. Hogeweg, J. Theor. Biol. 203 (2000) 317;
P. Hogeweg, Artif. Life 6 (2000) 85.
[11] C. Van Oss, A.V. Panfilov, P. Hogeweg, F. Siegert, C.J. Weijer, J. Theor. Biol. 181 (1996) 203.
[12] J.P. Rieu, A. Upadhyaya, J.A. Glazier, N.B. Ouchi, Y. Sawada, Biophys. J. 79 (2000) 1903.
[13] J.P. Rieu, N. Kataoka, Y. Sawada, Phys. Rev. E 57 (1998) 924.
[14] M. Sato-Maeda, M. Uchida, F. Graner, H. Tashiro, Dev. Biol. 162 (1994) 77.
[15] J.P. Rieu, Y. Sawada, Eur. Phys. J. B 27 (2002) 167.
[16] R.B. Dickinson, R.T. Tranquillo, AIChE J. 39 (1993) 1995.